Effects of physical ageing on creep in polypropylene

B. E. Read, G. D. Dean and P. E. Tomlins
Division of Materials Applications, National Physical Laboratory, Teddington, Middlesex, TW11 0LW, UK
(Received 21 April 1988; accepted 31 May 1988)

Creep data have been obtained for polypropylene at 23°C over an extensive time range (10^{-8}–10^{6} s) as a function of the elapsed time t_e between quenching from 80°C and the start of the creep experiment. The creep curves have been fitted with empirical functions capable of describing the behaviour across the entire β- and α-relaxation regions. Analyses of results from both short-term ($t \leqslant 0.1\, t_e$) and long-term tests suggest that physical ageing produces a decrease in relaxed compliance for the β-(glass–rubber) relaxation together with an increase in average retardation time and broadening of the α-process. Some decrease in magnitude of the α-relaxation also seems to be significant. It is proposed that ageing in polypropylene at room temperature could involve decreases in contour length of amorphous tie-molecules (yielding more extended conformations) through coupled motions in the crystalline and amorphous regions associated with the α-mechanism.

(Keywords: ageing; creep; polypropylene)

INTRODUCTION

Various empirical relationships have been proposed for describing the low-strain creep behaviour of polymers and these include a relatively versatile equation discussed by Struik[1,2] which takes the form

$$D(t) = D_0 \exp[(t/t_0)^{\gamma}] \qquad (1)$$

Here $D(t)$ is the tensile creep compliance, t_0 is related to some mean relaxation time and D_0 and γ are constants. Equation (1) with $\gamma \approx 1/3$ describes creep in glassy amorphous polymers at the short time end of the glass–rubber (α) relaxation[1]. It is then valid only for times t which are short compared with the physical age of the polymer as determined by the elapsed time t_e between a rapid cool from temperatures above the glass transition temperature T_g and the start of the creep test. This restriction arises from a marked increase in relaxation times, and hence t_0, for the glass–rubber relaxation with increasing age state. From a series of short-term tests ($t \leqslant 0.2\, t_e$) at different elapsed times the relationship between t_0 and t_e may be established[1]. It is then possible[1] to predict the creep behaviour in long-term experiments ($t \gg 0.2\, t_e$) when further ageing during the tests is progressively increasing t_0.

Since equation (1) predicts that the slopes of plots of $D(t)$ or log $D(t)$ against log t must increase indefinitely, it can only hold for times considerably shorter than the times at which inflexion points are observed in such plots from short-term tests. It is also applicable only when a single relaxation mechanism is responsible for the creep data. For the amorphous polymer PMMA, the longer time region of the secondary (β) relaxation process overlaps the initial stages of the glass–rubber (α) mechanism and short-term creep results at room temperature could not be described directly using equation (1). In this case[3,4] a range of dynamic mechanical experiments were used to obtain creep data at times spanned by the β-relaxation (10^{-8}–10 s). These results demonstrated that, unlike the α-mechanism, the creep response in the β region is independent of age state and may be successfully described by a function derived from the Cole–Cole equation[4]. The contribution to the creep compliance from the β-mechanism in the overlap region could then be predicted and the residual α-contribution could be described by equation (1). A subsequent prediction of the long-term creep behaviour using Struik's method compared reasonably well with experimental data[4].

Most partially crystalline polymers also exhibit overlapping relaxation regions which contribute to the creep response. The β-relaxation is usually ascribed to molecular motions in the bulk amorphous phase associated with the glass transition[5]. The α-process has been attributed to rearrangements of disordered segments close to the crystal surfaces which couple with motions within the crystals[6]. Struik has similarly suggested[7,8] that the α process involves motions of restrained amorphous segments in the vicinity of the crystals which give rise to an additional (upper) glass transition at a temperature T_g^u above T_g. On the basis of this model he has interpreted ageing effects over wide temperature ranges in terms of increases in retardation times for both the β and the α processes, corresponding to horizontal shifts of the component creep curves along the log time axis. However, ageing in semicrystalline polymers could give rise to changes in relaxation magnitude[8,9] rather than retardation times and such effects may, or may not, involve secondary crystallization.

In this paper, analyses are presented of creep data obtained for partially crystalline polypropylene after ageing for various times at room temperature. A combination of static and dynamic techniques was again employed to obtain results over a wide time range (10^{-8}–10^{6} s), which covered most of the β-relaxation and the early part of the α-relaxation. Short-term creep data are

0032-3861/88/122159-11$03.00

first analysed using functions which, unlike equation (1), may describe the behaviour across the entire β- and α-regions. The results of these analyses are then used in predicting the creep behaviour in long-term tests and the predictions are compared with long-term data obtained for the polymer at room temperature.

EXPERIMENTAL

Material

The polypropylene was obtained in the form of 12 mm thick sheets which were compression moulded by the supplier from granules of ICI Propathene GSE 16 homopolymer. Specimens machined from these sheets were annealed by heating to 130°C for 4 h followed by cooling to 23°C at 0.2°C min^{-1} to stabilize the crystallinity with respect to subsequent thermal treatments. The density of the annealed samples, determined by hydrostatic weighing in distilled water at 23°C, was 912 kg m^{-3}. The degree of crystallinity calculated from this density[10] was 71%.

Typical dimensions of the specimens used for creep measurements (10 × 10 × 160 mm) were larger than the dimensions of samples employed for the dynamic measurements (10 × 3 × 100 mm). However, creep tests conducted on a number of specimens of different cross-sectional area revealed no evidence of any structural heterogeneity through the specimen thickness.

Before the creep and dynamic mechanical measurements, the annealed specimens were heated to 80°C for 30 min, quenched in water at room temperature and then stored (aged) in air at 23°C for various periods of elapsed time t_e. The elapsed times ranged from 2.5 to 1200 h and the duration of each short-time creep test did not exceed 0.2 t_e. The reproducibility of the material ageing effects was investigated by repeating the thermal treatment at 80°C and the quenching and storage of several samples after completion of the creep measurements. Subsequent compliance values obtained for these samples agreed within experimental error (< 3%) with the original data for corresponding t_e values.

Measurement of creep compliance for times above 1 s

The apparatus used to obtain creep data at 23°C for $t \geqslant 1$ s has been described previously[11] and only a brief summary is given here. The specimen was located between two clamps. The lower clamp remained fixed and the upper clamp was constrained by a linear bearing such that the only permissible movement was along the long axis of the sample. Dead-weight loads (typically 60 N) were applied to the sample through the upper clamp via a pivoted arm having a 5:1 advantage. The extension of a sample under load was monitored by a pair of 50 mm gauge length extensometers located on opposite sides of the sample. Contact between each extensometer and the sample was via two knife edges, one attached to the body of an inductive transducer and the other to its core. Contact was maintained by a light pressure applied through the knife edges via a pair of spring steel clips.

The voltage outputs from the amplifier detecting each extensometer signal were sampled by a BBC microcomputer at selected time intervals ranging from 36 s to 10 h and stored on a magnetic disc. A transient recorder was used to make short time creep measurements at intervals of 0.1 s for the first 400 s after application of the load.

Compliance values obtained by this method for different samples of the same age generally agreed within 3%. The data presented in this paper are averages of $D(t)$ values obtained on four samples at each elapsed time.

Determination of creep compliance for times between 10^{-8} and 10 s

Values of creep compliance at short times covering the β-relaxation and initial part of the α-relaxation region for polypropylene were derived from measurements of the dynamic storage modulus E' and the loss modulus E'' over the frequency range 0.03 Hz–5 × 10^6 Hz at 23°C. The techniques employed have been discussed in previous publications[12,13] and comprised a tensile non-resonance method (0.03–100 Hz), an audiofrequency flexural resonance method (100 Hz–5 kHz) and an ultrasonic wave propagation technique (0.5–5 MHz). The storage moduli obtained by these methods are considered to be accurate to within 1%.

To obtain $D(t)$ values from the dynamic measurements it is convenient to specify the dynamic data in terms of the storage compliance $D'(\omega)$ and loss compliance $D''(\omega)$ as a function of angular frequency ω. These quantities are the components of the complex tensile compliance $D^*(\omega) = D'(\omega) - iD''(\omega)$, where $i = (-1)^{1/2}$, and may be obtained using $D^*(\omega) = 1/E^*(\omega)$ from the components of the complex modulus $E^*(\omega) = E'(\omega) + iE''(\omega)$. Since values of the loss factor $\tan\delta = D''/D'$ were < 0.15 at all frequencies studied for polypropylene, it follows that $D(t)$ values may be derived with an error less than 1.5% using the approximation[14]

$$D(t) = D'(1/t) + 0.337\, D''(0.323/t) \qquad (2)$$

where, as indicated, D' and D'' are evaluated at angular frequencies $1/t$ and $0.323/t$, respectively. The simpler approximation

$$D(t) = D'(\kappa/t) \qquad (3)$$

with the constant κ having a value of 0.63, was found to yield $D(t)$ values within 1% of those derived using equation (2) and was therefore employed in most data transformations.

ANALYSIS OF SHORT-TERM CREEP DATA IN THE β-RELAXATION REGION

Figure 1 shows creep curves covering up to 13 decades on the time scale for samples of different age and illustrates the good agreement between data obtained by the various methods. At times < 10^{-7} s the compliances derived from the ultrasonic data appear to lie on a short-time plateau whose level is essentially independent of t_e. With increasing time each creep curve exhibits a point of inflexion, corresponding to a mean retardation time for the β-mechanism around 10^{-5} s, a subsequent decrease in slope and a final increase in slope at times > 10^{-2} s. These results illustrate the dominance of the glass–rubber β-relaxation on the short-time compliance at room temperature and the onset of the overlapping α-process at longer times. At any given time, $D(t)$ decreases with increasing t_e.

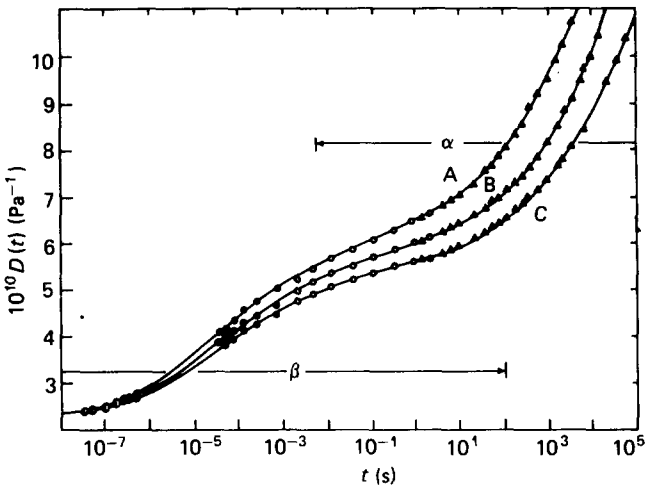

Figure 1 Creep curves for polypropylene at different states of physical ageing characterized by the elapsed time t_e after quenching from 80°C. A, $t_e = 2.5$ h; B, $t_e = 24$ h; C, $t_e = 216$ h. The techniques used to obtain the data were: ◐, ultrasonic wave propagation; ●, audio frequency flexural resonance; ○, tensile non-resonance; △, tensile creep. α and β indicate the timescales over which the α and β mechanisms are active

In analysing the creep behaviour in the β-relaxation region, it should first be recalled that equation (1) can only be valid at times short compared with the time corresponding to the point of inflexion. It could not therefore be used to describe the data over the entire β-region or to predict the β-compliance contribution in the region of overlap with the α-process.

In the β-region, the shapes of the $D(t) - \log t$ plots and corresponding $D' - \log \omega$ and $D'' - \log \omega$ curves are quite symmetrical. This observation is consistent with the fact that symmetrical Cole–Cole functions have been successfully used by Boyd[15] to fit dynamic mechanical data covering the α, β and γ regions of several semicrystalline polymers, including polypropylene. According to the Cole–Cole equation, the complex compliance for the β-relaxation is given by

$$D^*(\omega) = D_{U\beta} + \frac{\Delta D_\beta}{1 + (i\omega\tau_c)^n} \quad (4)$$

where: $\Delta D_\beta = D_{R\beta} - D_{U\beta}$, $D_{U\beta}$ and $D_{R\beta}$ being the unrelaxed and relaxed compliances for the β-process at limiting high and low frequencies, respectively; τ_c is an average retardation time for the β process; and n a parameter ($0 < n \leqslant 1$) characterizing the breadth of the β-retardation time spectrum. To obtain a corresponding relationship for $D(t)$ we now separate the real and imaginary components of equation (4) and transform to variable time using the approximation (3). This yields

$$D(t) = D_{U\beta} + D_\beta(t) \quad (5)$$

where $D_\beta(t)$ is the contribution to $D(t)$ from the β-process and may be written

$$D_\beta(t) = \Delta D_\beta \psi_{c\beta}(t) \quad (6)$$

where the normalized creep function $\psi_{c\beta}(t)$ is given by

$$\psi_{c\beta}(t) = \frac{(t/\kappa\tau_c)^n[(t/\kappa\tau_c)^n + \cos(n\pi/2)]}{1 + 2(t/\kappa\tau_c)^n \cos(n\pi/2) + (t/\kappa\tau_c)^{2n}} \quad (7)$$

According to equations (5)–(7) a plot of $D(t)$ against $\log t$ in the β-region is symmetrical about an inflexion point at time $\kappa\tau_c$. In fitting these equations to the short time data in *Figure 2* the τ_c value was obtained from experimental $D'' - \log \omega$ curves using $\omega_{max}\tau_c = 1$, where ω_{max} is the frequency of maximum D'' for the β-relaxation. This procedure follows from equation (4) and with $\kappa = 0.63$ yields $\kappa\tau_c = 3.15 \times 10^{-5}$ s. From the plots of D'' against $\log \omega$ for samples of different age state (*Figure 3*) it would appear that ω_{max}, and hence τ_c, for the β process does not change significantly with t_e. However, the magnitude of the D'' β-peak decreases substantially with increasing elapsed time.

Using the derived $\kappa\tau_c$ value, an optimization routine was employed to select values of $D_{U\beta}$, $D_{R\beta}$ and n such that the predicted creep curves (5) best fitted the experimental data over the time range 10^{-8}–10^{-3} s. Beyond this range the onset of the α-process yields an additional contribution to the measured compliance. The values of n and $D_{U\beta}$ were virtually constant at 0.30 and 2.0×10^{-10} Pa^{-1}, respectively, and, as illustrated in

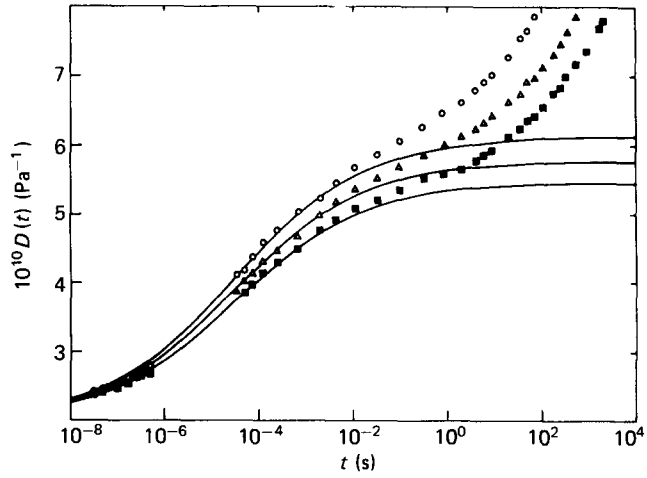

Figure 2 Modelling creep compliance through the β relaxation for samples of different age state using equations (5)–(7). t_e (h): ○, 2.5; △, 24; ■, 216; $\kappa\tau_c = 3.15 \times 10^{-5}$ s, $n = 0.30$, $D_{U\beta} = 2.0 \times 10^{-10}$ Pa^{-1}, ΔD_β is given by equation (8)

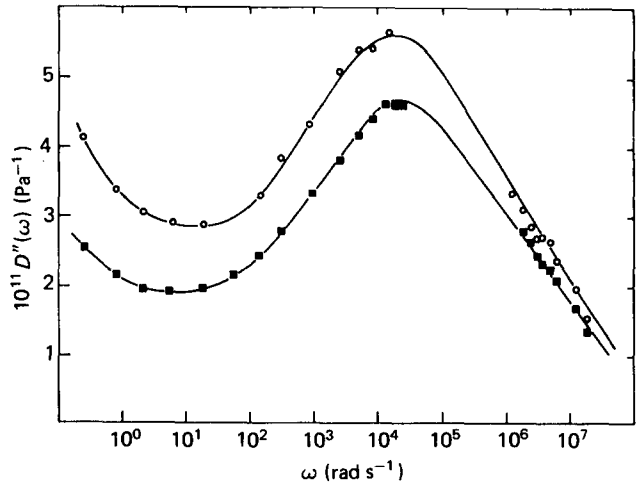

Figure 3 Imaginary compliance D'' as a function of angular frequency ω at elapsed times t_e of 2.5 h (○) and 216 h (■)

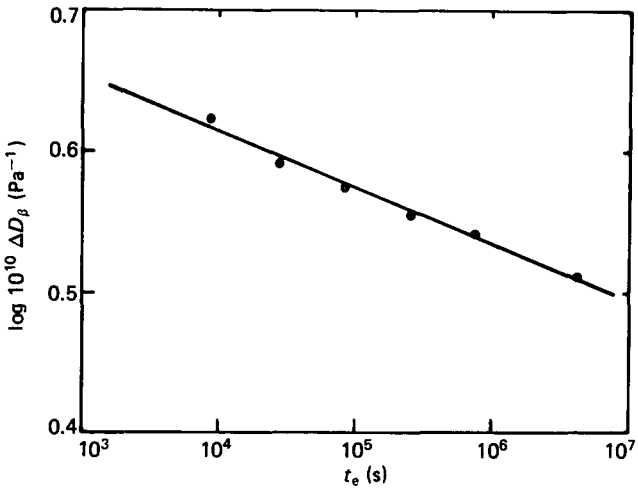

Figure 4 Log β-relaxation magnitude against log elapsed time, yielding $B=5.94\times10^{-10}\,Pa^{-1}\,s^k$ and $k=0.040$ in equation (8)

Figure 2, ageing effects in the β-region may be described almost entirely by a decrease in $D_{R\beta}$, and hence ΔD_β, with increasing t_e. A plot of log ΔD_β against log t_e was linear (*Figure 4*) and yielded the relationship

$$\Delta D_\beta = Bt_e^{-k} \tag{8}$$

for the elapsed time dependence of the β-relaxation magnitude. Values for the constants B and k were $5.94\times10^{-10}\,Pa^{-1}\,s^k$ and 0.040, respectively.

ANALYSIS OF SHORT-TERM CREEP IN THE α-RELAXATION REGION

At longer times when both the α and β-mechanisms contribute to the creep it is assumed that the total compliance may be written as

$$D(t)=D_{U\beta}+D_\beta(t)+D_\alpha(t) \tag{9}$$

where $D_\alpha(t)$ is the contribution to $D(t)$ from the α-process. In the region of time spanned by the α-relaxation the contribution $D_{U\beta}+D_\beta(t)$ may be predicted with the aid of equations (5)–(7) and $D_\alpha(t)$ thus obtained using equation (9) from the measured $D(t)$. Values of $D_\alpha(t)$ deduced in this way at various elapsed times are shown in *Figure 5*. The accuracy of these data is limited by the confidence with which the β-creep contribution can be extrapolated from short-time results. At the shorter times in *Figure 5* the $D_\alpha(t)$ values are very small and clearly prone to some error. However, the asymptotic approach of $D_\alpha(t)$ values to zero at short times provides some support for the validity of equations (5)–(7) in modelling the β-creep contribution.

From observations of the data in *Figure 5*, it is not possible to conclude whether the room temperature ageing in polypropylene is influencing the α-retardation times, as for the glass–rubber relaxation in amorphous polymers[1–4], or the α-relaxation magnitude, as observed for the β-mechanism in polypropylene. An attempt to fit the $D_\alpha(t)$ data using equation (1) was not very successful, a result ascribed partly to the fact that the longer creep times may not be substantially less than the inflexion time for the α-process. Furthermore, this equation does not permit variations in creep behaviour with age state to be partly described in terms of changes in relaxation magnitude.

Changes in either the relaxation magnitude or the relaxation time with ageing can be accounted for by an equation of the Cole–Cole form (equation (6)) and such a function is also consistent with the symmetrical forms of resolved α-relaxations of partially crystalline polymers as revealed by dynamic mechanical studies[15]. Before the application of the Cole–Cole equation, however, it is instructive to consider a relatively simple function of the Williams–Watts form[16] which, although yielding a non-symmetrical $D_\alpha(t)$ *versus* log t plot, can provide an accurate description of the $D_\alpha(t)$ data over the timescales so far investigated and can also account for changes in both relaxation magnitude and relaxation time with age state.

Application of a Williams–Watts function

In this treatment the contribution to $D(t)$ from the α-process is written

$$D_\alpha(t)=\Delta D_\alpha\{1-\exp[-(t/\tau_w)^m]\}=\Delta D_\alpha\psi_{w\alpha}(t) \tag{10}$$

where $\Delta D_\alpha=D_{R\alpha}-D_{U\alpha}$, $D_{R\alpha}$ and $D_{U\alpha}$ being the relaxed and unrelaxed compliances, τ_w is related to some mean retardation time for the α-process and m is a parameter ($0<m\leqslant1$) characterizing the breadth of the retardation-time distribution. Note that equation (10) is consistent with a creep recovery function of the form $\exp[-(t/\tau_w)^m]$ and hence with the analogous function proposed by Williams and Watts to describe the charge decay associated with the primary relaxation in amorphous polymer dielectrics. The exponential term may be expanded as a power series to give

$$\frac{D_\alpha(t)}{\Delta D_\alpha}=\left(\frac{t}{\tau_w}\right)^m\left[1-\frac{1}{2}\left(\frac{t}{\tau_w}\right)^m+\ldots\right] \tag{11}$$

so that when $(t/\tau_w)^m\ll1$ it follows that

$$\log D_\alpha(t)=\log\Delta D_\alpha+m\log t-m\log\tau_w \tag{12}$$

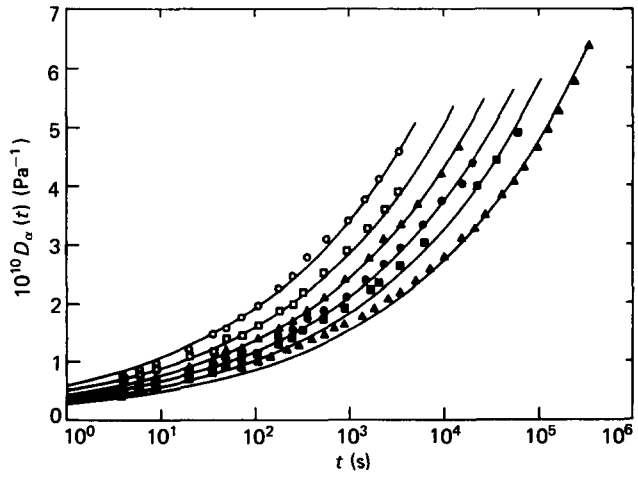

Figure 5 Short-term creep data for the α-relaxation mechanism at different elapsed times t_e (h): ○, 2.5; □, 8; △, 24; ●, 72; ■, 216; ▲, 1200. The solid lines are given by equation (15) with $P=21.4\times10^{-10}\,Pa^{-1}$, $Q=444\times10^{-10}\,Pa^{-1}\,s^r$, $r=0.211$, $\tau_w=3\times10^8$ s and $m=0.255$

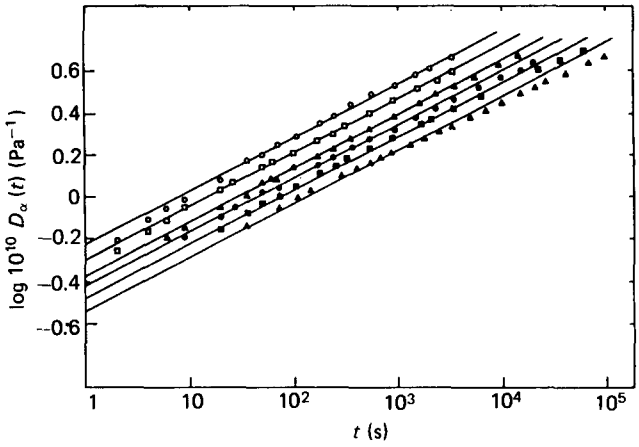

Figure 6 Log α-creep compliance against log time at different elapsed times t_e. The straight lines correspond to a constant value for the distribution parameter $m=0.255$. Symbols are explained in *Figure 5*

and a plot of $\log D_\alpha(t)$ against $\log t$ will be linear with slope m.

The experimental data in *Figure 5* are shown as double logarithmic plots in *Figure 6*. *For* $t < 10^3$ s the variation of $\log D_\alpha(t)$ with $\log t$ is linear within experimental error. There is a clear indication that the gradient in this time range decreases slightly with elapsed time, suggesting a small decrease in m over the t_e range studied. However, in an attempt to simplify the data analysis, the consequences are first investigated of assuming that m takes a constant average value. Data analyses will subsequently be presented where the small variations in m are considered.

Case 1: m constant. The straight line fits shown in *Figure 6* correspond to a gradient $m=0.255$, representing an average value for the gradients of the lines best fitting the data (*Figure 7*). It is apparent that with increasing t the data exhibit negative deviations from the lines in *Figure 6* at a time which is essentially independent of age state. From equation (11), this observation suggests that τ_w is independent of elapsed time and therefore implies that the influence of physical ageing on creep behaviour in the α-region involves predominantly changes in the relaxation magnitude ΔD_α. If the data deviate by 2% from the straight lines at a time t_c then equation (11) yields

$$\tau_w = t_c/0.04^{1/m} \tag{13}$$

and taking $t_c \approx 10^3$ s we obtain $\tau_w \approx 3 \times 10^8$ s. Values for ΔD_α corresponding to each elapsed time curve were then deduced using equation (12) from the intercepts at $\log t = 0$. An empirical relationship of the form

$$\Delta D_\alpha = P + Q t_e^{-r} \tag{14}$$

was found to describe the elapsed time dependence of ΔD_α. Values for $P = 21.4 \times 10^{-10}\ Pa^{-1}$, $Q = 444 \times 10^{-10}\ Pa^{-1}\ s^r$ and $r = 0.211$ were obtained using an optimization routine.

Equations (14) and (10) now yield

$$D_\alpha(t) = (P + Q t_e^{-r})\{1 - \exp[-(t/\tau_w)^m]\} \tag{15}$$

for the contribution from the α-mechanism to short-term creep in polypropylene. Using the derived values for the parameters, predicted curves of $D_\alpha(t)$ against $\log t$ from equation (15) are compared with experimental data in *Figure 5*. The agreement is within experimental error.

Case 2: m variable. Figure 7 shows the same data as *Figure 6* but the gradients of the linear fits at short times are no longer taken to be constant but to decrease as indicated with increasing t_e. This trend corresponds to a decrease in m with elapsed time which can be described quite accurately by the relationship

$$m = m_0 t_e^{-\chi} \tag{16}$$

with $m_0 = 0.358$ and $\chi = 0.027$ and implies a slight broadening of the distribution of retardation times for the α-mechanism with increasing age.

It is also apparent from *Figure 7* that the decrease in m is accompanied by an increase in the time at which the departure from linearity occurs. According to equation (11) these combined trends are consistent with the assumption that τ_w increases with elapsed time. The deviations from linearity in *Figure 7* are not sufficiently well defined to obtain an accurate value of t_c and hence τ_w at each elapsed time. However, assuming that ΔD_α is constant, the variation of τ_w with t_e was derived as follows. At an arbitrary elapsed time of 72 h, a 2% deviation from linearity was found to occur at $t_c \approx 10^3$ s. From the gradient $m = 0.258$ of the 72 h plot, an approximate τ_w value of 2.6×10^8 s was then obtained using (13) and an estimate of $\Delta D_\alpha = 53 \times 10^{-10}\ Pa^{-1}$ was subsequently determined from the intercept at $\log t = 0$ (equation (12)). Assuming that this ΔD_α value is independent of t_e, the τ_w values at other elapsed times were then deduced from the relevant intercepts and slopes, again using equation (12). A plot of $\log \tau_w$ against $\log t_e$ is linear, as shown in *Figure 8*, implying an ageing relationship for τ_w of the form

$$\tau_w = A t_e^{\mu} \tag{17}$$

with $A = 1.66 \times 10^4\ s^{1-\mu}$ and $\mu = 0.77$.

The appropriate equation for modelling the short-term creep contribution from the α-mechanism now becomes (compare equation (15)),

$$D_\alpha(t) = \Delta D_\alpha\{1 - \exp[-(t/A t_e^{\mu})^{m_0 t_e^{-\chi}}]\} \tag{18}$$

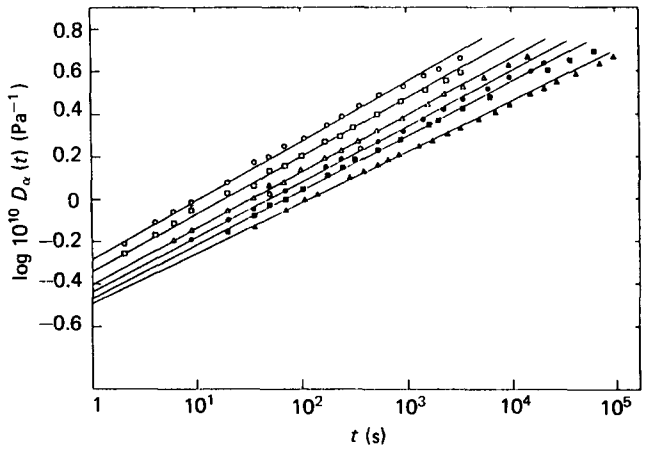

Figure 7 As for *Figure 6* except that the gradient m is now allowed to vary with elapsed time. Values for t_e (h) and optimum values for m are, respectively, ○, 2.5, 0.278; □, 8, 0.272; △, 24, 0.265; ●, 72, 0.258; ■, 216, 0.250; ▲, 1200, 0.238

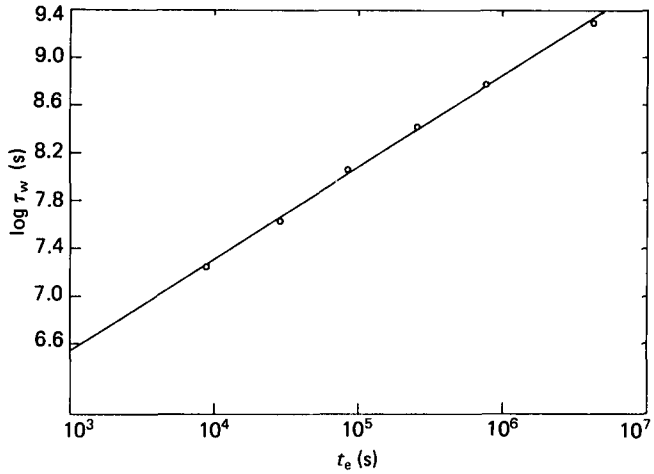

Figure 8 Log α-retardation time *versus* log elapsed time, yielding $A=1.66\times10^4\,s^{1-\mu}$ and $\mu=0.77$ in equation (17)

Curves derived from this equation are compared with experimental data in *Figure 9*. The agreement is just as satisfactory as that in *Figure 5*.

Use of a Cole–Cole function

An analysis similar to that in the previous section can be developed on the basis of the Cole–Cole function. Applying equations of the form of equations (6) and (7) to the α-relaxation, and noting that $\cos(n\pi/2)$ has a value close to unity for $0.2\leqslant n\leqslant0.3$, we obtain for small $(t/\kappa\tau_c)^n$ the approximation

$$\frac{D_\alpha(t)}{\Delta D_\alpha}\approx\left(\frac{t}{\kappa\tau_c}\right)^n\left[\cos\frac{n\pi}{2}+\left(\frac{t}{\kappa\tau_c}\right)^n\right]\left[1-2\left(\frac{t}{\kappa\tau_c}\right)^n\cos\frac{n\pi}{2}\right]$$

$$=\left(\frac{t}{\kappa\tau_c}\right)^n\cos\frac{n\pi}{2}\left[1-\left(2\cos\frac{n\pi}{2}-\frac{1}{\cos(n\pi/2)}\right)\left(\frac{t}{\kappa\tau_c}\right)^n+\ldots\right] \quad (19)$$

where τ_c and n now refer to the α-process. When $(t/\kappa\tau_c)^n\ll1$ it follows that

$$\log D_\alpha(t)=\log\Delta D_\alpha+n\log t-n\log\kappa\tau_c+\log\cos(n\pi/2) \quad (20)$$

so that the plot of $\log D_\alpha(t)$ against $\log t$ is again predicted to be linear, as observed in *Figure 6*, with slope $n=m$. Deviations of 2% from linearity in these plots now occur at a critical time t_c given by

$$1-\left[2\cos\frac{n\pi}{2}-\frac{1}{\cos(n\pi/2)}\right]\left(\frac{t_c}{\kappa\tau_c}\right)^n=0.98 \quad (21)$$

Derivation of the parameters for modelling the influence of physical ageing on short-term creep in polypropylene therefore follows the same procedures as described in the section above on the Williams–Watts function but employing equations (6), (20) and (21) in place of equations (10), (12) and (13), respectively. For Case 1 in *Figure 6*, where $n=m=0.255$ and τ_c are considered constant, $\kappa\tau_c$ was found to be 1.5×10^9 s and the variation in ΔD_α with elapsed time could be described using equation (14) with $P=34.7\times10^{-10}\,Pa^{-1}$, $Q=715\times10^{-10}\,Pa^{-1}\,s^r$ and $r=0.209$. With these parameters, equations of the form of equations (6) and (7) yield curves virtually identical to those from equation (15) in *Figure 5* for times up to about $10^{7.5}$ s. Over this time range it is assumed that the Cole–Cole and Williams–Watts functions with different but corresponding parameters will give very similar predictions for Case 2 above and under other conditions.

LONG-TERM CREEP BEHAVIOUR

In the short-term creep experiments discussed above, the age of each specimen was essentially constant since the creep times were considerably less than t_e. With longer term tests, further ageing during the period under load must be considered in the prediction of long-term behaviour. The short-term results suggest that further ageing during room temperature creep in polypropylene will affect the long-term compliance through changes in parameters characteristic of both the β- and α-relaxations. For the β-relaxation, the ageing will give rise to a progressive decrease in magnitude ΔD_β but have a negligible effect on the mean retardation time and distribution parameter. For the α-process, changes may occur either in ΔD_α or in the mean retardation time and the distribution. Following these observations, we now analyse the long-term creep on the basis of a viscoelastic model which can account for changes either in the relaxation magnitude or in the retardation times. Details of the model and calculations are given in the Appendix.

Case 1: ΔD_α variable, τ_w and m constant

When ΔD_β and ΔD_α are each reduced by the ageing, and all retardation times are unaffected, the long-term creep compliance is given by equation (A11), which may be written in the form

$$D(t)=D_{U\beta}+\Delta D_\beta(0)\psi_\beta(t)+\Delta D_\alpha(0)\psi_\alpha(t)+I_\beta+I_\alpha \quad (22)$$

The first three terms on the right-hand side of this equation describe the short-term creep at constant $\Delta D_\beta(0)$ and $\Delta D_\alpha(0)$, which are the relaxation magnitudes at the start of the creep test. The integrals I_β and I_α represent

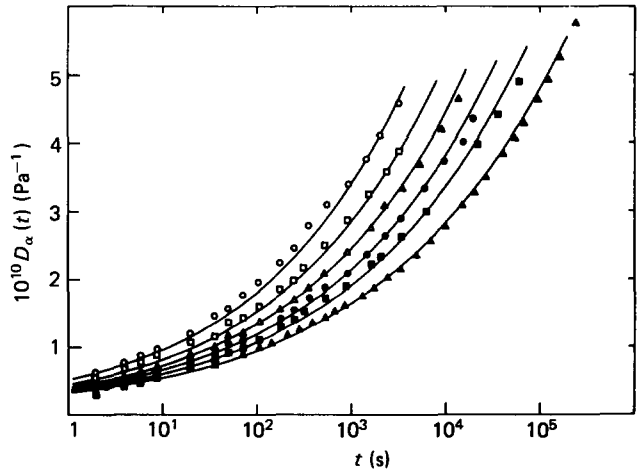

Figure 9 Comparison of data for the short-term creep contribution from the α-relaxation at several elapsed times t_e with predicted curves given by equation (18). $A=1.66\times10^4\,s^{1-\mu}$, $\mu=0.77$, $\Delta D_\alpha=53\times10^{-10}\,Pa^{-1}$, $m_0=0.358$ and $\chi=0.027$. Symbols are explained in *Figure 5*

Table 1 Values for the integrals I_α and I_β in equation (22) determined by numerical integration of equation (A11)[a]

	$-10^{10} I_\beta$ (Pa^{-1})			$-10^{10} I_\alpha$ (Pa^{-1})		
t (s)	t_e=8 h	t_e=24 h	t_e=72 h	t_e=8 h	t_e=24 h	t_e=72 h
1×10^4	0.05	0.02	0	0.13	0	0
3×10^4	0.11	0.04	0.02	0.52	0.16	0.04
6×10^4	0.17	0.08	0.03	0.94	0.36	0.10
1×10^5	0.23	0.11	0.05	1.47	0.60	0.19
3×10^5	0.36	0.22	0.11	2.90	1.50	0.64
6×10^5	0.46	0.30	0.17	4.22	2.34	1.14
1×10^6	0.52	0.36	0.22	5.25	3.18	1.69
3×10^6	0.67	0.50	0.35	8.34	5.34	3.22
6×10^6	0.75	0.59	0.43	10.6	7.03	4.50
1×10^7	0.82	0.65	0.49	12.2	8.4	5.56
3×10^7			0.61			8.34

[a] $Q=444\times10^{-10}$ Pa^{-1} s^r, $r=0.211$, $\tau_w=3\times10^8$ s

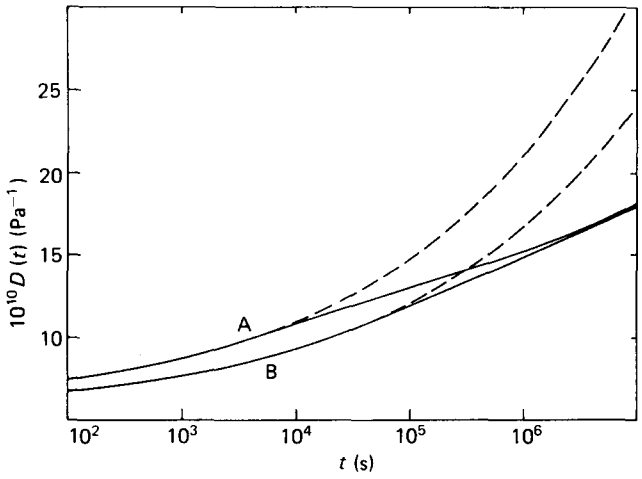

Figure 10 Comparison of long-term creep behaviour predicted using equation (22) (———) with extrapolated short-term curves (– – –) given by the first three terms of equation (22). m and τ_w are assumed constant. The parameters used in the calculation are given in *Figures 2, 4* and *5* and *Table 1*. A, t_e=8 h; B, t_e=72 h

negative contributions to $D(t)$ arising from the reductions in ΔD_β and ΔD_α due to further ageing.

In applying equation (22), we let $\psi_\beta(t)=\psi_{c\beta}(t)$ and $\psi_\alpha=\psi_{w\alpha}(t)$, bearing in mind that $\psi_{c\beta}(t)$ is characterized by constant τ_c and n and that $\psi_{w\alpha}(t)$ is associated with constant τ_w and m. From equations (8) and (14) we then substitute the following into equation (22):

$$\begin{aligned}\Delta D_\beta(0)&=Bt_e^{-k}\\ \Delta D_\beta(u)&=B(t_e+u)^{-k}\\ \Delta D_\alpha(0)&=P+Qt_e^{-r}\\ \Delta D_\alpha(u)&=P+Q(t_e+u)^{-r}\end{aligned}\qquad(23)$$

Using values for the parameters given above, the integrals I_β and I_α have been evaluated numerically. Values are given in *Table 1* at discrete times t corresponding to long-term creep experiments for the elapsed times considered here. The magnitudes of I_α and I_β become significant at times $t>t_e/3$ and this criterion therefore defines the limit of short-term tests for polypropylene according to this model. It can be seen that I_α has much larger negative values than I_β.

Long-term creep curves predicted using equation (22) are compared in *Figure 10* with extrapolated short term curves given by the first three terms in equation (22). This plot demonstrates the substantial influence that physical ageing has on long-term creep behaviour, the vertical difference between curves at the same elapsed time representing the term $I_\alpha+I_\beta$. *Figure 11* compares long-term predicted curves with experimental data at three elapsed times. It is apparent that the influence of ageing is to reduce creep rates such that curves at different age states converge at long times. Although this feature is observed in the experimental data, predictions are consistently below measured values, the agreement being better at 72 h elapsed time than at 8 h.

To investigate the scope for obtaining better predictions of long-term creep behaviour using this model, alternative parameters were considered in the analysis of short-term data. The selection of a higher value for $\tau_w=1\times10^9$ s gave rise to the need for revised estimates for ΔD_α and hence P and Q in equation (14). New values for I_α were also evaluated. The predicted long-term creep curves had slightly higher gradients, resulting in a small improvement in the agreements with data, although insufficient to justify confidence in the model.

The use of the Cole–Cole function, equation (6), in place of the Williams–Watts function to model creep in the α region was also investigated. The parameters employed are given in the section on the Cole–Cole function above and new values for I_α again had to be computed. Long-term creep predictions were made using equation (22) but now the function $\psi_\alpha(t)$ took the form of the Cole–Cole function, equation (7). These predictions were indistinguishable from those made using the Williams–Watts function shown in *Figure 11* and, therefore, again lie significantly below measured values.

Case 2: τ_w and m variable, ΔD_α constant

The analysis of short-term data in the α-region has been described above for the case where ΔD_α is assumed constant and both τ_w and m vary with t_e. To allow for these effects, together with decreases in ΔD_β, in the prediction of long-term creep we now employ equation (A13) from the Appendix. The creep function $\psi_\beta(t)$ is

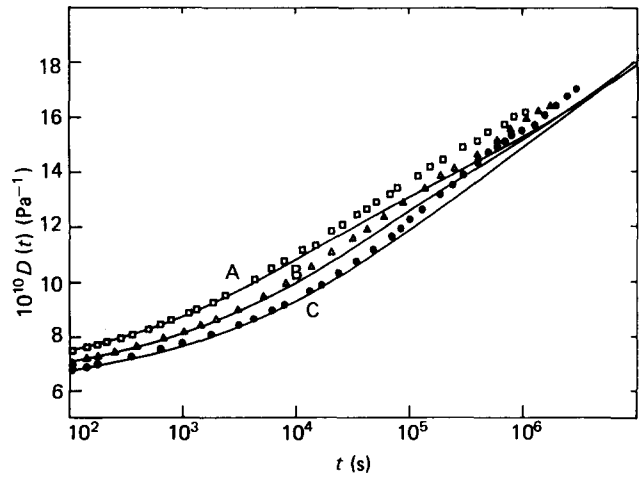

Figure 11 Comparison of long-term creep data at three elapsed times with curves predicted using equation (22). Parameters are the same as in *Figure 10*. A, t_e=8 h; B, t_e=24 h; C, t_e=72 h

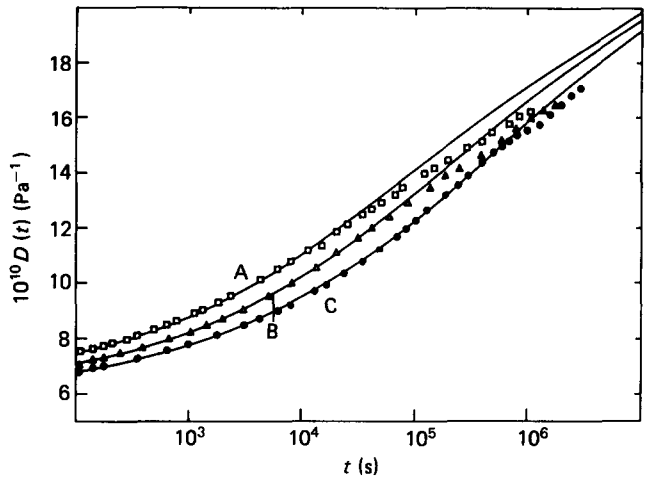

Figure 12 Comparison of long-term creep data with curves predicted using equation (27) in which m and τ_w vary with time. Parameters are given in *Figures 2* and *9* and *Table 1*. A, $t_e=8$ h; B, $t_e=24$ h; C, $t_e=72$ h

again identified with $\psi_{c\beta}(t)$ and, for the generalized creep function $\psi_{\lambda\alpha}(t)$, we write

$$\psi_{\lambda\alpha}(t)=1-\exp[-(\lambda_w(t)/\tau_w(0))^{m(t)}] \tag{24}$$

where, following (A4) and (17),

$$\lambda_w(t)=\int_0^t\frac{\tau_w(0)}{\tau_w(\xi)}d\xi=\int_0^t\left(\frac{t_e}{t_e+\xi}\right)^{\mu}d\xi \tag{25}$$

and, from (16), $m(t)$ is given by

$$m(t)=m_0(t_e+t)^{-\chi} \tag{26}$$

In comparing (24) with the definition of $\psi_{\lambda\alpha}(t)$ in (A8) we note that the effective time $\lambda(t,\tau(0))$ in (A8) replaces the real time t to account for the increasing retardation times during long-term creep and that the broadening of the distribution arises from a dependence of $\lambda(t,\tau(0))$ on $\tau(0)$. In the empirical function (24) the increasing retardation times are allowed for by replacing t with the effective time $\lambda_w(t)$ which relates to the mean retardation time τ_w. The broadening of the distribution is then characterized by the time dependence of m.

Equation (A13) may now be written

$$D(t)=D_{U\beta}+\Delta D_\beta(0)\psi_{c\beta}(t)+I_\beta$$
$$+\Delta D_\alpha\left\{1-\exp\left[-\left(\frac{t_e^{1-\mu}}{A(1-\mu)}[(1+t/t_e)^{1-\mu}-1)\right)^{m_0(t_e+t)^{-\chi}}\right]\right\} \tag{27}$$

Long-term creep curves obtained using equation (27) are compared with experimental data in *Figure 12*. A convergence in creep behaviour at longer times is predicted by this equation but occurs more slowly than observed in the data. Furthermore, calculated long-term creep compliances lie significantly above experimental values, especially at the shorter elapsed times. To investigate the influence of alternative estimates of retardation times, values for $\tau_w=7\times10^7$ s and 1×10^9 s at $t_e=72$ h were also considered (cf. $\tau_w=2.6\times10^8$ s at $t_e=72$ h in *Figure 12*). New values (assumed constant) for ΔD_α were calculated and the dependence of τ_w on t_e could again be described by equation (17) with appropriate new values of μ and A. The predicted long-term creep curves became lower and closer to the experimental curves with decreasing τ_w. However, at the shortest τ_w studied the convergence of predicted curves was still slower than that found experimentally.

It is apparent that predictions of long-term creep based on Case 2 (*Figure 12*) tend to overestimate the compliances and yield a late convergence of creep curves, whereas predictions based on Case 1 (*Figure 11*) underestimate compliances and give an early convergence of curves. Although the Case 2 predictions are closer to the experimental data, these observations suggest that a more realistic model should describe ageing effects partly in terms of an increasing τ_w but with an additional simultaneous reduction in ΔD_α. With such a general model, difficulties are anticipated in separating experimentally the contributions from the two sources.

DISCUSSION

In discussing the structural origins of the above results we first note that the heat treatment at 80°C and storage at 23°C are unlikely to induce changes in crystallinity for material annealed at 130°C. Hence the structural changes during ageing at 23°C almost certainly occur in the amorphous phase. The nature of these changes, and their influence on the creep data, may be considered initially in terms of Struik's model[8]. For this purpose the β- and α-relaxations will be associated with the respective lower and upper transition temperatures T_g^L and T_g^U within the proposed distribution of T_g. Here T_g^L is the normal glass transition temperature (T_g) of the more mobile, unconstrained amorphous material and T_g^U the glass transition temperature of less mobile amorphous material which is close to, and constrained by, the crystals. According to Struik's model the structural changes during ageing mostly involve molecular rearrangements of the kind associated with the glass transitions and can yield decreases in mobility of both the less mobile and the more mobile amorphous regions. At high ageing temperatures some secondary crystallization effects are also proposed which have little influence on molecular mobility. In discussing the effect of these changes on the creep of semicrystalline polymers, Struik distinguished between the observed behaviour in four different temperature regions (Regions 1–4).

For polypropylene at 20°C, Struik reported that short-term, semi-logarithmic creep curves ($4\leqslant t\leqslant10^4$ s) obtained at different elapsed times could be superposed by downward vertical shifts together with horizontal shifts to longer times. He interpreted this result in terms of his 'Region 2' type behaviour, employing a geometrical construction (Reference 8, Figure 6(b)) of questionable validity. Our data in *Figures 1* and *2* suggest, in fact, that $D_\beta(t)$ for the more mobile material is approaching its rubbery plateau at creep times above 1 s and that the creep data should be considered, therefore, in relation to Region 3 ($T_g^L<T<T_g^U$). According to Struik's model the downward shift in creep curves, which corresponds to our decrease in ΔD_β with t_e, might then be ascribed to a reduction in the quantity of more mobile material. The horizontal shift would be attributed to a decrease in

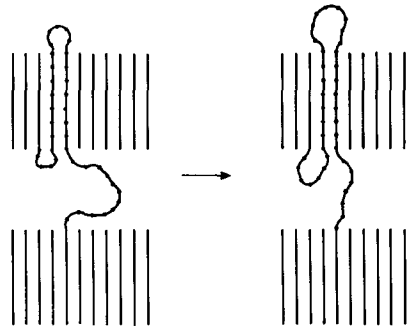

Figure 13 Schematic illustration of a possible ageing mechanism associated with the α-process

mobility of the less mobile regions, equivalent to our increase in $\tau_{w\alpha}$ with t_e.

Although such interpretations are broadly consistent with our observations, they raise further difficulties. First, an upward vertical shift is suggested by Struik for Region 3 which is opposite to that observed. Secondly, it is difficult to understand how the amount of more mobile material decreases with elapsed time since it is at equilibrium immediately after quenching. The slight broadening of the α-region (decrease in m) with t_e indicated by our data, and the possible decrease in ΔD_α, further suggest that the superposition of creep curves by combinations of vertical and horizontal shifts will not be strictly valid, as found by Chai and McCrum[17].

In considering other possible ageing mechanisms in polypropylene, we assume that the slow underlying structural changes at room temperature involve conformational rearrangements of the type responsible for the α-retardation process. However, on the basis of much existing evidence, we accept that the α-process may not be associated with an upper T_g but originates from segmental motions in the amorphous phase which couple with the translation of polymer chains along the c crystal axes[6,18]. *Figure 13* illustrates how such motions could decrease the contour length of a tie-molecule linking neighbouring crystals, through the lengthening of loops on the crystal surfaces. Since this process should yield a decreased number of bonds in high-energy rotational states then, at equilibrium with respect to the α-mechanism and in the absence of an external stress, the average length of tie-molecules will decrease with decreasing temperature. Following a rapid quench from a high temperature to some lower temperature T within the α-region, the contour lengths of tie-molecules will therefore decrease (at a rate controlled by the α-retardation time at T) as the polymer seeks a new equilibrium structure. Owing to the constraints produced by the crystals, the tie-molecules will thus slowly assume more extended conformations relative to those existing in equilibrium at higher temperatures. For such a process to be feasible, it must of course produce a decrease in free energy. Thus the conformational entropy decrease arising from the tie-molecule extensions, which would yield a positive contribution to the free energy change, must be outweighed by other contributions such as a decrease in internal energy and increase in entropy of the folds. An increased resistance to deformation (at intermediate timescales of loading) resulting from the increased tie-molecule extensions might then account for the decrease in $D_{R\beta}$ with elapsed time. The high calculated values of amorphous-phase rubbery moduli for semi-crystalline polymers are in fact consistent with the suggestion of extended molecules in the amorphous layers[6,19].

The observed increase in α-retardation time with t_e further requires that the activation energy for creep increases with the structural changes during ageing. Assuming that the barriers hindering the motions of amorphous segments contribute to the activation energy, this could result from the increased population of bonds in low-energy states. Regarding these tentative suggestions, it should be added that a small increase in crystal lamellar thickness due to secondary crystallization (although considered unlikely) might also yield significant increases in tie-molecule extension[19] and in activation energy for the α-process[6]. We finally note that physical ageing in glassy amorphous polymers also involves decreases both in conformational entropy and enthalpy in the approach to a more ordered equilibrium structure[20]. Further work is being undertaken to assess the validity of the various models.

CONCLUSIONS

Accurate creep data for polypropylene may be obtained over 14 decades of time t using a combination of static and dynamic techniques. Results obtained at 23°C cover the glass–rubber β-relaxation region (10^{-8}–10^{2} s) and the onset of the overlapping α-process at times $> 10^{-2}$ s. The data exhibit a marked dependence on the physical age of the polymer as determined by the elapsed time t_e at 23°C between quenching from 80°C and the start of the creep.

Curves of creep compliance $D(t)$ against $\log t$ in the β-region are quite well fitted by a symmetrical Cole–Cole function, enabling reliable estimates to be obtained (by extrapolation) of the compliance contributions from the β- and α-processes in the overlap region. Results of this analysis show that the magnitude ΔD_β, or relaxed compliance $D_{R\beta}$, of the β-process decreases with t_e and that the mean retardation time and distribution of retardation times for the β process are essentially unaffected by ageing.

In the case of short-term experiments ($t \leqslant 0.1\, t_e$), the creep compliance contribution from the α-process at the times so far studied (up to 10^6 s) may be described by functions of the Williams–Watts or the Cole–Cole form. Within experimental error, the influence of ageing on short-term creep can be accounted for by either (Case 1) a decrease in magnitude ΔD_α with elapsed time and no change in retardation times or (Case 2) an increase in average retardation time with t_e together with some broadening of the distribution at constant ΔD_α.

Predictions of long-term creep behaviour are possible with the aid of a phenomenological model which can account for changes either in relaxation magnitude or retardation times due to ageing processes accompanying the creep. Discrepancies are observed between experimental long-term creep curves and predicted curves based either on Case 1 or Case 2. Although the Case 2 predictions show a closer agreement with experiment, these observations suggest that ageing gives rise both to increases in α-retardation times and to some decrease in ΔD_α.

The results of this investigation do not fully support Struik's model of ageing in partially crystalline polymers, which is based on the concept of a distribution of glass

temperatures for the amorphous phase. It is suggested that ageing in polypropylene at room temperature is controlled by the α-process. This involves cooperative rearrangements in the crystalline and amorphous regions and might yield gradual decreases in contour length, and thus more extended conformations, of amorphous tie-molecules after quenching from high temperatures.

APPENDIX: PHENOMENOLOGICAL MODEL FOR LONG-TERM CREEP

We first consider, for a given relaxation process, the ith element of a generalized Voigt model (*Figure 14a*) subjected to a constant stress σ_c for times $t \geq 0$. If $\varepsilon_i(u)$ is the strain in the element at time u between 0 and t the compliance contribution $D_i(u) = \varepsilon_i(u)/\sigma_c$ is given by[5]

$$\frac{dD_i(u)}{du} + \frac{D_i(u)}{\tau_i(u)} = \frac{\Delta D_i(u)}{\tau_i(u)} \tag{A1}$$

Here $\tau_i(u)$ is the retardation time of the element and $\Delta D_i(u)$ its contribution to the total compliance increment $\Delta D(u)$ associated with the given relaxation region. Note that both $\tau_i(u)$ and $\Delta D_i(u)$ may vary with time u owing to further ageing during the creep experiment. We now multiply each side of (A1) by the integrating factor $\exp[\int_0^u d\xi/\tau_i(\xi)]$ where ξ is a time variable. Integrating from $u=0$ to t with $D_i(0)=0$ we then obtain

$$D_i(t)\exp\left[\int_0^t \frac{d\xi}{\tau_i(\xi)}\right] = \int_0^t \frac{\Delta D_i(u)}{\tau_i(u)} \exp\left[\int_0^u \frac{d\xi}{\tau_i(\xi)}\right] du \tag{A2}$$

which yields, after some manipulation,

$$D_i(t) = \int_0^t \frac{\Delta D_i(u)}{\tau_i(u)} \exp\left[-\frac{\lambda_i(t) - \lambda_i(u)}{\tau_i(0)}\right] du \tag{A3}$$

Here $\lambda_i(t)$ and $\lambda_i(u)$ are 'effective times' given by

$$\lambda_i(t) = \int_0^t \frac{\tau_i(0)}{\tau_i(\xi)} d\xi$$
$$\lambda_i(u) = \int_0^u \frac{\tau_i(0)}{\tau_i(\xi)} d\xi \tag{A4}$$

and $\tau_i(0)$ is the retardation time at the start of the creep test. Since $d\lambda_i(u)/du = \tau_i(0)/\tau_i(u)$ it follows from (A3) that

$$D_i(t) = \int_0^t \Delta D_i(u) \frac{d}{du} \exp\left[-\frac{\lambda_i(t) - \lambda_i(u)}{\tau_i(0)}\right] du \tag{A5}$$

The total compliance $D(t)$ is now obtained by summing the contributions from all elements. In the limit of a continuous distribution we obtain

$$D(t) = -\int_0^t \Delta D(u) \frac{d}{du} \psi_\lambda(t,u) du \tag{A6}$$

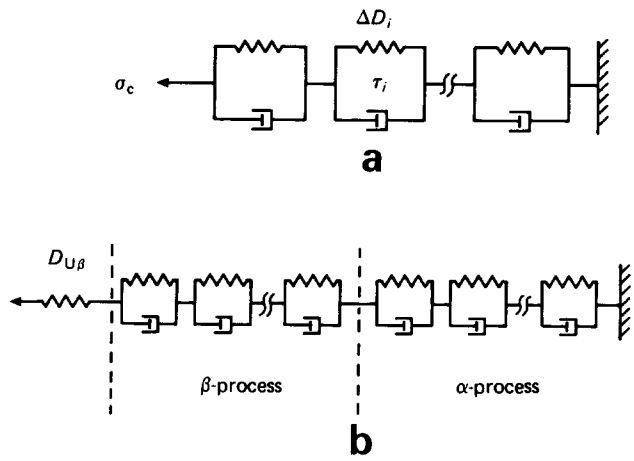

Figure 14 Generalized Voigt models for (a) a given relaxation process and (b) two overlapping processes α and β with an instantaneous component

where

$$\psi_\lambda(t,u) = \int_0^\infty \phi(\tau(0)) \left\{1 - \exp\left[-\frac{\lambda(t,\tau(0)) - \lambda(u,\tau(0))}{\tau(0)}\right]\right\} d\tau(0) \tag{A7}$$

and $\phi(\tau(0))$ is the normalized distribution of retardation times at the start of the creep. Note that the dependence of the effective times $\lambda(t,\tau(0))$ and $\lambda(u,\tau(0))$ on $\tau(0)$ allows for changes in the breadth of the retardation time distribution with further ageing during creep. Furthermore for $u=0$, $\lambda(u,\tau(0))$ vanishes and (A7) becomes

$$\psi_\lambda(t) = \int_0^\infty \phi(\tau(0)) \left\{1 - \exp\left[-\frac{\lambda(t,\tau(0))}{\tau(0)}\right]\right\} d\tau(0) \tag{A8}$$

Integration of (A6) by parts then yields

$$D(t) = \Delta D(0)\psi_\lambda(t) + \int_0^t \psi_\lambda(t,u) \frac{d}{du} \Delta D(u)\, du \tag{A9}$$

where $\Delta D(0)$ is the value of $\Delta D(u)$ at the instant of loading.

The creep behaviour arising from overlapping α- and β-mechanisms may now be analysed by an extension of the above model. For this purpose we consider a generalized Voigt model (*Figure 14b*) containing distributions of elements representative of each process in series with a spring to account for the instantaneous compliance $D_{U\beta}$ assumed to be unaffected by ageing. It follows that

$$D(t) = D_{U\beta} + \Delta D_\beta(0)\psi_{\lambda\beta}(t) + \int_0^t \psi_{\lambda\beta}(t,u) \frac{d}{du} \Delta D_\beta(u)\, du$$
$$+ \Delta D_\alpha(0)\psi_{\lambda\alpha}(t) + \int_0^t \psi_{\lambda\alpha}(t,u) \frac{d}{du} \Delta D_\alpha(u)\, du \tag{A10}$$

where subscripts α and β are used to denote the

magnitudes and creep functions ψ_λ of the respective processes.

Equation (A10) accounts for the effects on long-term creep of changes produced by ageing both in the relaxation magnitudes and in the relaxation times and distribution of relaxation times (which influence the ψ_λ). Considerable simplification arises if changes occur either in the magnitude or in the relaxation times for a given process. If, for example, the ageing yield decreases in the magnitudes ΔD_β and ΔD_α and if the relaxation times for both the α- and β-relaxations are unaffected so that $\lambda(t,\tau(0))=t$ and $\lambda(u,\tau(0))=u$ for each process, then (A10) becomes

$$D(t)=D_{U\beta}+\Delta D_\beta(0)\psi_\beta(t)+\int_0^t \psi_\beta(t-u)\frac{\mathrm{d}}{\mathrm{d}u}\Delta D_\beta(u)\,\mathrm{d}u \qquad (A11)$$

$$+\Delta D_\alpha(0)\psi_\alpha(t)+\int_0^t \psi_\alpha(t-u)\frac{\mathrm{d}}{\mathrm{d}u}\Delta D_\alpha(u)\,\mathrm{d}u$$

The creep functions

$$\psi_\beta(t)=\int_0^\infty \phi_\beta(\tau)[1-\exp(-t/\tau)]\,\mathrm{d}\tau$$

and (A12)

$$\psi_\alpha(t)=\int_0^\infty \phi_\alpha(\tau)[1-\exp(-t/\tau)]\,\mathrm{d}\tau$$

may be identified with empirical functions such as $\psi_c(t)$ and $\psi_w(t)$ above, yielding relationships[21] between the $\phi(\tau)$ and parameters τ_c and n or τ_w and m.

If the ageing produces a decrease in ΔD_β and changes in α-relaxation times and distribution of relaxation times for the α-process, and both the β-relaxation times and ΔD_α are unaffected, then (A10) reduces to

$$D(t)=D_{U\beta}+\Delta D_\beta(0)\psi_\beta(t)+\int_0^t \psi_\beta(t-u)\frac{\mathrm{d}}{\mathrm{d}u}\Delta D_\beta(u)\,\mathrm{d}u$$

$$+\Delta D_\alpha\psi_{\lambda\alpha}(t) \qquad (A13)$$

ACKNOWLEDGEMENTS

The authors wish to acknowledge the assistance of Mr M. R. Wells with the collection and analysis of some of the creep data and of Mrs A. Woolf with the use of the optimization routine.

REFERENCES

1 Struik, L. C. E. 'Physical Ageing of Amorphous Polymers and Other Materials', Elsevier, Amsterdam, 1978
2 Struik, L. C. E. in 'Failure of Plastics' (Eds. W. Brostow and R. D. Corneliussen), Hanser, Munich, 1986, ch. 11, p. 209
3 Read, B. E. in 'Molecular Dynamics and Relaxation Phenomena in Glasses' (Eds. Th. Dorfmüller and G. Williams), *Lecture Notes in Physics* **277**, Springer-Verlag, Berlin, 1987, p. 61
4 Dean, G. D., Read, B. E. and Small, G. D. *Plast. Rubber Process. Appl.* 1988, **9**, 173
5 McCrum, N. G., Read, B. E. and Williams, G. 'Anelastic and Dielectric Effects in Polymeric Solids', Wiley, London, 1967
6 Boyd, R. H. *Polymer* 1985, **26**, 1123
7 Struik, L. C. E. *Plastics Rubber Process. Appl.* 1982, **2**, 41
8 Struik, L. C. E. *Polymer* 1987, **28**, 1521
9 Chai, C. K. and McCrum, N. G. *Polymer* 1984, **25**, 291
10 Miller, R. L. in 'Encyclopedia of Polymer Science and Technology', Vol. 4 (Ed. N. Bikales), Wiley, New York, 1966
11 Read, B. E. and Dean, G. D. *Polymer* 1984, **25**, 1679
12 Read, B. E. and Dean, G. D. 'The Determination of Dynamic Properties of Polymers and Composites', Adam Hilger, Bristol, 1978
13 Read, B. E., Dean, G. D. and Duncan, J. C. in 'Physical Methods of Chemistry' (Eds. B. W. Rossiter, J. F. Hamilton and R. C. Baetzold), Wiley–Interscience, New York, Vol. VII, ch. 1, to be published
14 Schwarzl, F. R. and Struik, L. C. E. *Adv. Mol. Relaxation Processes* 1968, **1**, 201
15 Boyd, R. H. *Polymer* 1985, **26**, 323
16 Williams, G. and Watts, D. C. *Trans. Faraday Soc.* 1970, **66**, 80
17 Chai, C. K. and McCrum, N. G. *Polymer* 1980, **21**, 706
18 McCrum, N. G. in 'Molecular Basis of Transitions and Relaxations' (Ed. D. J. Meier), *Midland Macromol. Inst. Monographs* No. 4, 1978, p. 167
19 Krigbaum, W. R., Roe, R.-J. and Smith, Jr, K. J. *Polymer* 1964, **5**, 533
20 Matsuoka, S. *Polym Eng. Sci.* 1981, **21**, 907
21 Lindsey, C. P. and Patterson, G. D. *J. Chem. Phys.* 1980, **73**, 3348